Lasers in Manufacturing Conference 2023

Online determination of the local hardness during laser beam welding of steel

David Traunecker[a,*], Michael Jarwitz[a], Andreas Michalowski[a], Thomas Graf[a]

[a]*Institut für Strahlwerkzeuge, University of Stuttgart, Pfaffenwaldring 43, Stuttgart 70569, Germany*

Abstract

Due to the increasing product variety, flexible production facilities are required that can already work productively from batch-size 1 onwards. This requires flexible and online-capable quality assurance of the processes to be able to detect defective parts as soon as possible.
One important quality feature in laser welding is the resulting hardness, which usually must be determined post-process. In this paper, a method for the spatially resolved online determination of the hardness is presented at the example of laser welding of mild steel. The dependence of the hardness on the cooling rate was utilized for this purpose.
Therefore, the cooling curves were determined spatially resolved during the welding process using a scanning pyrometer and the heat loss coefficient was determined from these cooling curves as a measure of the cooling rate. The corresponding local hardness was determined post-process. The results show a correlation between the local hardness values and the local heat loss coefficients within a set of process parameters, making this a promising approach for the spatially resolved online determination of the hardness.

Keywords: process monitoring; online monitoring; temperature measurement; hardness; laser beam welding

1. Introduction

Today's production systems have to face major challenges as they have to continuously move to a more sustainable production and simultaneously work productively from batch-size 1 onwards. For this, defective products have to be detected as soon as possible, which leads to the need for automatic and reliable quality assurance of manufacturing processes, such as laser beam welding. In particular, in-process quality assurance is necessary to increase productivity, Gonzalez-Val et al., 2020. However, this is a major challenge, since for most manufacturing processes the quality cannot yet be measured in-process, Thombansen et al., 2018.

* Corresponding author. Tel.: +49 711 685 66877
E-mail address: David.traunecker@ifsw.uni-stuttgart.de.

Several types of defects can occur during laser beam welding. For defects that are visible from the surface, such as a false capillary depth and excess weld metal, an in-process measurement of the surface geometry can be used e.g. with an OCT (optical coherence tomography) system, Dupriez and Truckenbrodt, 2016, Webster et al., 2014. However, the in-process detection of internal defects, such as pores and the estimation of the microstructure, are still major challenges.

The microstructure of the weld seam and the resulting hardness can also be used as an indicator for other mechanical properties, Keehan, 2004, Pavlina and Van Tyne, 2008. Usually, the hardness has to be determined using hardness indentations. This is very time-consuming since the samples have to be prepared, the hardness measurements require a certain amount of time, and afterward, the samples are destroyed. It is known that the cooling rate of the weld seam influences the microstructure and the properties of the weld seam, Bhadeshia and Svensson, 1993. This relation was used, for example, to actively tune the hardness of the produced samples during the laser-based powder bed fusion process of AlSi10Mg by adjusting the cooling rate through the process parameters, Leis et al., 2022. The heat loss coefficient describes the cooling process, DIN EN ISO 11551:2020-05, and therefore can be used as a simplified measure of the cooling rates. The heat loss coefficient is determined by an exponential fit to the cooling curves, DIN EN ISO 11551:2020-05.

In the present work, the feasibility of using the heat loss coefficient for an in-process estimation of the local hardness is investigated. For this purpose, a scanning pyrometer is used to measure the temperature fields during the laser welding process.

2. Experimental setup and data processing

Experiments were carried out to investigate the correlation between the heat loss coefficient and the hardness. The schematic experimental setup is shown in Fig. 1.

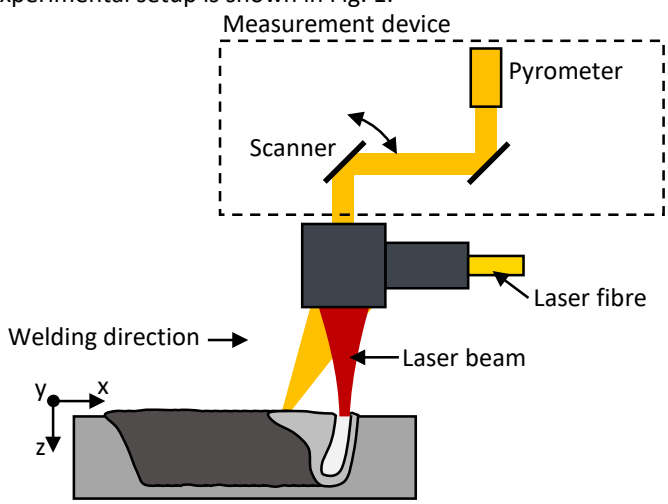

Fig. 1, Schematic view of the experimental setup with a longitudinal section of the laser beam welding process, the welding direction, the laser beam, the laser fiber, and the self-built measurement device, which was connected to the laser optics.

A disk laser TruDisk 16002 with a wavelength of 1030 nm was used as the laser source. The used laser fiber has a diameter of 200 mm and the beam parameter product after the fiber is 10 mm*mrad. A focusing optics with a focal length of 200 mm for the collimation and focusing lens was used. Additionally, the laser beam was defocused by +1 mm, which resulted in a beam diameter of approximately 280 µm on the surface of the sample. The optics was tilted by 5° to avoid direct back reflections. For the protection of the optics, the spatters were blown away in the welding direction using compressed air. The used material is structural steel S235.

The varied process parameters were the laser power and the feed rate, which resulted in four different parameters, which were repeated three times. The four parameter sets are shown in Table 1

Table 1. Used process parameters.

	Laser power in W	Feed rate in m/min
Parameter set 1	2000	2
Parameter set 2	4000	2
Parameter set 3	6000	2
Parameter set 4	4000	10

During the laser welding process, the temperature was measured spatially resolved using a pyrometer and a self-built scanning system. After the process, the surface hardness of the samples was measured. The used self-built measurement device allows connecting a pyrometer and to move the measurement spot independently from the laser beam with the integrated scanner. The analog data of the actual position of the scanner and the measured temperature values of the pyrometer were recorded and synchronized using a measurement card NI USB-6361 from National Instruments with a measurement frequency of 35 kHz. In Fig. 2 the scan field, which was scanned meander-shaped by the scanner, and the hatch distance *h* is shown in a schematic top-view illustration of the laser beam welding process.

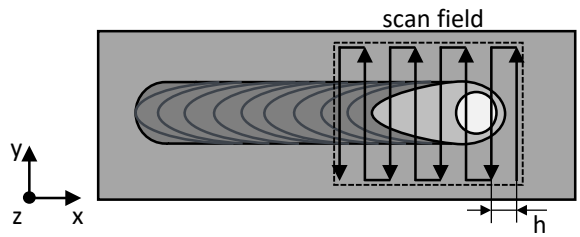

Fig. 2. Schematic top-view illustration of a laser beam welding process, with the meander shaped scan field surrounded by the dotted black rectangle and the hatch distance *h*.

The scan field had dimensions of 11.4 mm in the x-direction and 5.2 mm in the y-direction. For the slow parameter of 2 m/min, the scan velocity was approximately 1630 mm/s, and the hatch distance was around 160 µm. For the fast parameter of 10 m/min, the scan field was shifted by -3 mm in the x-direction, the scan velocity was approximately 2400 mm/s, and the hatch distance *h* was 240 µm. The movement of the scanner started before the start of the welding process and stopped after the end of the welding process. Therefore, the scan field was scanned multiple times during the welding process. The number of runs of the scan field during the welding process depends on the feed rate and the scan parameter. At least 4 complete temperature fields could be measured during each welding process.

The diameter of the measurement spot of the pyrometer in the processing plane was approximately 300 µm. Due to the acceleration of the scanner, the measurement points are not uniformly distributed inside the scan field. Therefore, a grid with the same dimension as the scan field and a grid size of 100 µm was generated, to further evaluate the spatially resolved temperature field. The values on the grid were defined by the nearest measurement data point. It was assumed that the feed rate of the welding process is constant and the temperature field during the process, besides the beginning and the end of the process, is in a steady state. An example of a resulting temperature field is shown as an image in Fig. 3 a). In Fig. 3 b) the temperature

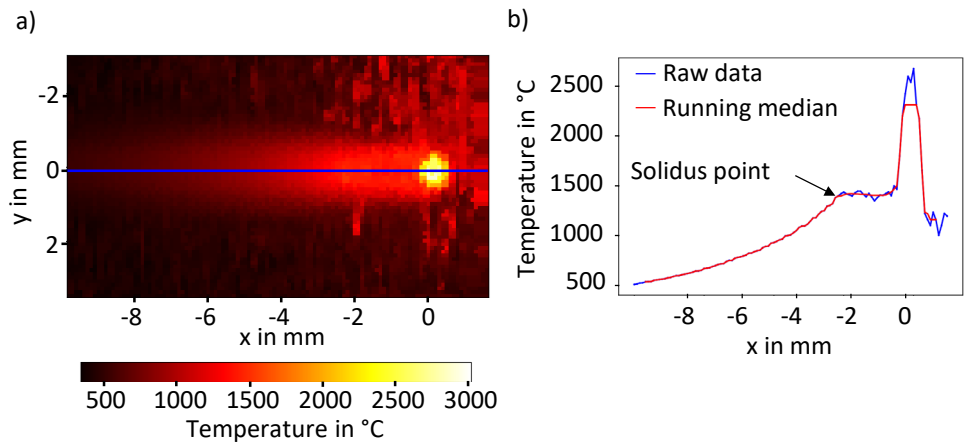

Fig. 3. Example of a temperature field measured during a welding process with P = 2 kW and v = 2 m/min. a) generated image of the temperature field from the scanner and pyrometer data; b) temperature data at the position y = 0 as a function of x from the example temperature field shown in (a). The red curve represents the filtered temperature data from a running median of nine data points. The end of the melt pool is shown by the solidus point.

data at the position y = 0 of the image in Fig. 3 a) is shown (represented by the blue line). The red curve shows the data filtered with a running median of nine data points.

In the first step, cooling curves had to be derived from the acquired temperature data, to be able to derive a heat loss coefficient from the measurements. For this, the temperature data were taken at the desired y-position. Secondly, the data were filtered with a running median of nine data points to remove noise and high-temperature fluctuations caused by spatters. In the next step, the cooling curves had to be transformed into temperature data as a function of time, as the cooling curves were derived from the spatially resolved temperature field. With the already mentioned assumption that the temperature field is in a steady state, the scan velocity in the negative x-direction can be used to transform the x-position to the time. The scan velocities in the -x-direction are for the slow scan parameter 37.2 ± 0.24 mm/s and the fast scan parameter 101.1 ± 0.66 mm/s. These velocities were directly determined from the actual position data of the scanner. The fourth step was to carry out an exponential fit to the cooling curve and determine the heat loss coefficient from it. For this, the start and end point of the exponential fit had to be determined. The endpoint of the fit was in all cases the end of the measured temperature data. The starting point depended on whether the cooling curve temperature data was on or adjacent to the weld seam. If the data was on the weld seam, the start point was set to the solidus point. If the data was not on the weld seam, the start point was set to the point where a dropping cooling curve was visible. With the value of the exponent of the exponential function of the fit curve, the heat loss coefficient can be determined. In Fig. 4 the temperature data from Fig. 3 b) after the solidus point is shown as a function over time. The red dotted line represents the exponential fit with the function parameters and the coefficient of determination given in the graph. The heat loss coefficient is framed in red.

The steps described for determining the heat loss coefficient were carried out at different y-positions of the same temperature field and different temperature fields of the same welding process. At least 4 temperature fields of the same welding process were investigated, which results in 12 heat loss coefficients for every investigated y-position for every parameter set.

After the welding process, the surface of the samples was ground and polished to get a flat surface for the measurement of the hardness, which was carried out using the Carat 930 from ATM GmbH. The hardness measurements were carried out according to Vickers with HV0.5, DIN EN ISO 6507-1:2018-07. It is assumed

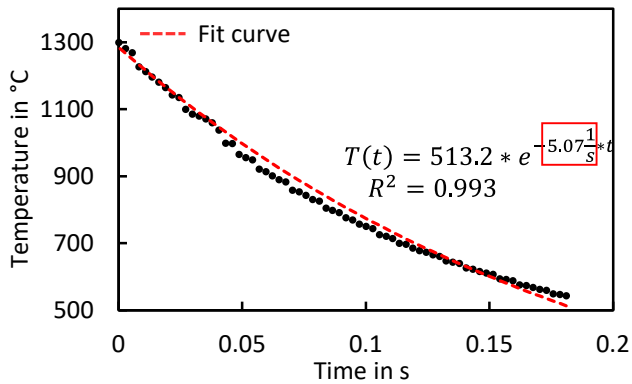

Fig. 4. Temperature data as a function of the time for the data already shown in Fig. 3 b). The red dashed line represents the exponential fit to the cooling curve. The function parameters and the coefficient of determination of the fit are given in the graph. The heat loss coefficient is framed in red.

that changes in hardness occur only in the y-direction and that in the welding direction, the hardness is nearly constant. Two different hardness measurements were performed, one with a constant distance of the hardness indentations in the y-direction of 300 µm and the other with a distance of 500 µm, for both 11 indentations per row were performed. To cover the whole welding seam and to keep the measurement time within limits, the distance of the hardness indentations in the x-direction was set to 2 mm. This results in at least an amount of around 17 hardness values for each investigated y-position of every sample and a total of around 51 hardness values for each parameter set for every y-position.

3. Results

In Fig. 5 the measured hardness is shown as a function of the heat loss coefficient for the 4 investigated sets of process parameters. The different data points within a set of process parameters are from different y-positions. For each data point, the markers show the average values of all measurements examined at this y-position, and the error bars indicate the standard deviation.

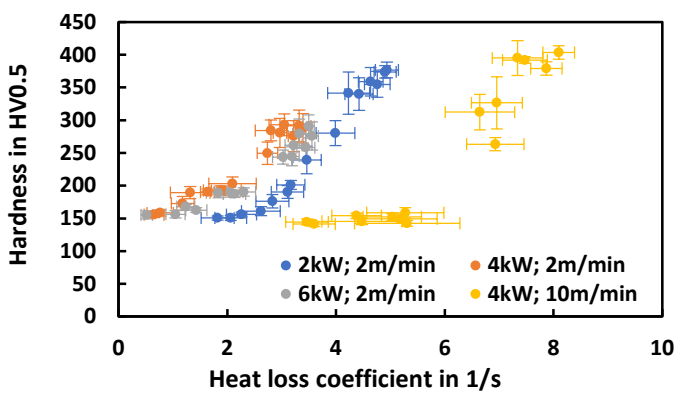

Fig. 5. Hardness in HV0.5 as a function of the heat loss coefficient in 1/s for different process parameters.

It can be seen, that the hardness increases for higher heat loss coefficients within one set of process parameters, which indicates a correlation between the hardness and the heat loss coefficient within one set of process parameters. However, depending on the process parameters, the value of the heat loss coefficient

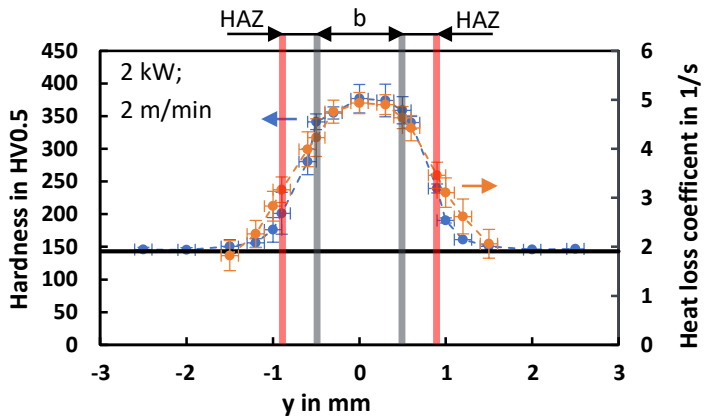

Fig. 6. Hardness in HV0.5 and heat loss coefficient in 1/s as a function of y for the laser parameters P = 2 kW and v = 2 m/min. The black horizontal line represents the hardness of the basic microstructure without any heat influence from the laser beam welding process. Also, the width of the weld seam b, and the heat affected zone (HAZ) are shown depending on the y-position.

can be different for the same value of the hardness, which indicates that the hardness is also dependent on another variable, which needs further investigation.

In Fig. 6 the hardness and the heat loss coefficient are shown as a function of the y-position for a laser power of 2 kW and a feed rate of 2 m/min. The hardness of the base material without any heat influence is represented by the black horizontal line, which was measured on a separate sample.

It can be seen, that the hardness increases before and within the heat-affected zone (HAZ) and, within the weld seam until the highest hardness is reached in the middle of the weld seam, which is at position y = 0. The same can be seen for the heat loss coefficient. This shows again the correlation between the heat loss coefficient and the hardness on the surface of the sample. For the other parameters which were investigated the same behavior between the heat loss coefficient and the hardness could be seen. Therefore, it is assumed that the heat loss coefficient is a suitable tool to estimate the local hardness from the temperature data measured during the process. It should be noted, that at the current state, the correlation between the heat loss coefficient and the hardness has to be determined for each set of process parameters.

4. Conclusion

In this work, the correlation between the heat loss coefficient and the hardness on the surface was investigated to estimate the local hardness at different y-positions with the heat loss coefficient. The temperature fields were measured using a scanning pyrometer and with further data processing, the cooling curves were determined, which were used to determine the heat loss coefficient by an exponential fit. The evaluated data show a correlation between the hardness and the heat loss coefficient within a set of process parameters. Therefore, it is possible to estimate the local hardness using the heat loss coefficient. However, there is an influence of the process parameters on the correlation between the hardness and the heat loss coefficient, so the same coefficient can lead to a different hardness for a different process parameter. For the investigation of this influence, further research is necessary.

Acknowledgements

The presented work was funded by the Ministry of Science, Research and the Arts of the Federal State of Baden-Wuerttemberg within the „Innovation Campus Future Mobility“, which is gratefully acknowledged.

References

Dupriez, Nataliya Deyneka; Truckenbrodt, Christian (2016) OCT for Efficient High Quality Laser Welding. In : Laser Technik Journal, vol. 13, n° 3, p. 37–41. DOI: 10.1002/latj.201600020.

DIN EN ISO 11551:2020-05, Optics and photonics - Lasers and laser-related equipment - Test method for absorptance of optical laser components (ISO 11551:2019, Corrected version 2020-01); German version EN ISO 11551:2019.

DIN EN ISO 6507-1:2018-07, Metallic materials - Vickers hardness test - Part 1: Test method (ISO 6507-1:2018); German version EN ISO 6507-1:2018.

Gonzalez-Val, Carlos; Pallas, Adrian; Panadeiro, Veronica; Rodriguez, Alvaro (2020) A convolutional approach to quality monitoring for laser manufacturing. In: Journal of Intelligent Manufacturing, vol. 31, n° 3, p. 789–795. DOI: 10.1007/s10845-019-01495-8.

H. Bhadeshia; L. Svensson (1993) Modelling the Evolution of Microstructure in Steel Weld Metal. Mathematical Modelling of Weld Phenomena, eds Cerjak, H., Easterling E.K., Institute of Materials, London, pp. 109–182.

Keehan, E. (2004) Effect of Microstructure on Mechanical Properties of High Strength Steel Weld Metals, Department of Experimental Physics Chalmers University of Technology, Göteborg

Leis, Artur; Traunecker, David; Weber, Rudolf; Graf, Thomas (2022) Tuning the Hardness of Produced Par ts by Adjusting the Cooling Rate during Laser-Based Powder Bed Fusion of AlSi10Mg by Adapting the Process Parameters. In: Metals, vol. 12, n° 12, p. 2000. DOI: 10.3390/met12122000.

Pavlina, E., Van Tyne, C. (2008) Correlation of Yield Strength and Tensile Strength with Hardness for Steels. In: J. of Materi Eng and Perform 17, 888–893. https://doi.org/10.1007/s11665-008-9225-5

Thombansen, Ulrich; Buchholz, Guido; Frank, Daniel; Heinisch, Julian; Kemper, Maximilian; Pullen, Thomas et al. (2018) Design framework for model-based self-optimizing manufacturing systems. In: International Journal of Advanced Manufacturing Technology, vol. 97, n° 1-4, p. 519–528. DOI: 10.1007/s00170-018-1951-8.

Webster, P. J. L.; Wright, L. G.; Ji, Y.; Galbraith, C. M.; Kinross, A. W.; van Vlack, C.; Fraser, J. M. (2014) Automatic laser welding and milling with in situ inline coherent imaging. In: Optics Letters, vol. 39, n° 21, p. 6217. DOI: 10.1364/ol.39.006217.